EUROPEAN ORGANIZATION FOR NUCLEAR RESEARCH

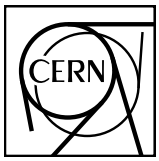

ALICE-PUBLIC-2015-008

Centrality dependence of the charged-particle multiplicity density at midrapidity in Pb-Pb collisions at $\sqrt{s_{\rm NN}}$ = 5.02 TeV

ALICE Collaboration*

Abstract

This note provides additional material related to the analysis of mid-rapidity pseudorapidity density of charged particles ($\langle {\rm d}N_{\rm ch}/{\rm d}\eta \rangle$) in Pb–Pb collisions at a centre-of-mass energy per nucleon pair, $\sqrt{s_{\rm NN}}$ = 5.02 TeV (arXiv:1512.06104). We discuss the details of the Glauber Monte Carlo calculation, and its relation with the experimental data, including the application of the extended Glauber model, which uses quarks as sub-nuclear degree of freedom. We also present the comparison of the current results with the $\langle {\rm d}N_{\rm ch}/{\rm d}\eta \rangle$ measurement at $\sqrt{s_{\rm NN}}$ = 2.76 TeV, with a discussion on the systematic uncertainties.

*The author list is given in arXiv:1512.06104.

1 Introduction

This note provides additional material related to the analysis of mid-rapidity pseudorapidity density of charged particles ($\langle \mathrm{d}N_{\mathrm{ch}}/\mathrm{d}\eta \rangle$) in Pb–Pb collisions at a centre-of-mass energy per nucleon pair, $\sqrt{s_{\mathrm{NN}}}$ = 5.02 TeV. In Section 2, we give some details on the Glauber model used by ALICE. We extract mean numbers of the relevant geometrical quantities for typical centrality classes defined by classifying the events according to their impact parameter. We describe the determination of the fraction of the hadronic cross section used for analysis, which determines the absolute scale of the centrality via a fit based on the Glauber model. We compare the mean number of participants for centrality classes selected by the impact parameter to those selected in the fitted multiplicity distribution. We discuss different particle production mechanism that can be employed in the parameterization of $\langle \mathrm{d}N_{\mathrm{ch}}/\mathrm{d}\eta \rangle$. This also includes the application of the extended Glauber model, which uses quarks as sub-nuclear degree of freedom. In Section 3, we discuss the dependence of $\frac{2}{\langle N_{\mathrm{part}} \rangle} \langle \mathrm{d}N_{\mathrm{ch}}/\mathrm{d}\eta \rangle$ on the center-of-mass energy, by comparing the data at $\sqrt{s_{\mathrm{NN}}}$= 5.02 TeV to the same measurement performed at $\sqrt{s_{\mathrm{NN}}}$= 2.76 TeV in LHC Run 1.

2 Glauber Monte Carlo

Table 1 provide mean numbers of the relevant geometrical quantities, calculated using the ALICE Glauber Monte Carlo [1], for different centrality classes defined by classifying the events according to their impact parameter.

The nucleon position in the ^{208}Pb nucleus is determined by the nuclear density function, modeled by the functional form (modified Woods-Saxon or 2-parameter Fermi distribution):

$$\rho(r) = \rho_0 \frac{1 + w(r/R)^2}{1 + \exp\left(\frac{r-R}{a}\right)} \tag{1}$$

Protons and neutrons are assumed to have the same nuclear profile. The parameters used for the calculation are:

- ρ_0 is the nucleon density, which provides the overall normalization, not relevant for the Monte Carlo simulation,
- $R = (6.62 \pm 0.06)$ fm is the radius parameter of the ^{208}Pb nucleus and
- $a = (0.546 \pm 0.010)$ fm is the skin thickness of the nucleus, which indicates how quickly the nuclear density falls off near the edge of the nucleus
- w is needed to describe nuclei whose maximum density is reached at radii $r > 0$ ($w = 0$ for Pb).
- $d_{\mathrm{min}} = 0.4$ fm a hard-sphere exclusion distance of between the centers of the nucleons, i.e. no pair of nucleons inside the nucleus has a distance less than d_{min}. The hard-sphere exclusion distance, characteristic of the length of the repulsive nucleon-nucleon force, is not known experimentally and thus is varied by 100% ($d_{\mathrm{min}} = (0.4 \pm 0.4)$ fm).
- $\sigma_{\mathrm{NN}}^{\mathrm{inel.}}$ = (70 ± 5) mb for nuclear collisions at $\sqrt{s_{\mathrm{NN}}} = 5.02$ TeV, we use as in [2], estimated by interpolation of pp data at different center-of-mass energies and from cosmic rays [3, 4], and subtracting the elastic scattering cross section from the total cross section.

The total Pb–Pb cross section is calculated as $\sigma_{\mathrm{PbPb}} = (7.72 \pm 0.22(syst.))$ b.

The systematic uncertainties on the mean values are obtained by independently varying the parameters of the Glauber model within their estimated uncertainties.

Centrality	b_{min} (fm)	b_{max} (fm)	$\langle N_{part} \rangle$	RMS	(*sys.*)	$\langle N_{coll} \rangle$	RMS	(*sys.*)	$\langle T_{pPb} \rangle$ 1/mbarn	RMS 1/mbarn	(*sys.*) 1/mbarn
00 – 10 %	0.00	4.96	359	31.2	3.0	1640	246	170	23.4	3.51	0.78
10 – 20 %	4.96	7.01	263	27.1	3.6	1000	154	97	14.3	2.2	0.46
20 – 30 %	7.01	8.59	188	22.5	3.0	601	106	54	8.59	1.52	0.27
30 – 40 %	8.59	9.92	131	19.1	2.3	344	74.7	29	4.92	1.07	0.16
40 – 50 %	9.92	11.1	86.3	16.3	1.7	183	50.8	14	2.61	0.726	0.1
50 – 60 %	11.1	12.1	53.6	13.6	1.2	89.8	32.4	6	1.28	0.463	0.063
60 – 70 %	12.1	13.1	30.4	10.8	0.76	39.8	19.1	2.4	0.569	0.273	0.032
70 – 80 %	13.1	14.0	15.6	7.83	0.45	16.2	10.5	0.92	0.232	0.15	0.015
80 – 90 %	14.0	15.0	7.59	4.89	0.19	6.46	5.27	0.3	0.0923	0.0753	0.007
90 – 100 %	15.0	19.6	3.77	2.5	0.079	2.65	2.41	0.088	0.0378	0.0344	0.0033
0 - 1 %	0.00	1.56	405	4.61	1.5	2030	88.5	210	29.0	1.26	0.98
1 - 2 %	1.56	2.22	396	6.21	2.1	1930	85.4	200	27.6	1.22	0.91
2 - 3 %	2.22	2.71	386	7.49	2.7	1830	80.9	190	26.2	1.16	0.87
3 - 4 %	2.71	3.13	375	8.51	3.0	1740	77.3	180	24.9	1.10	0.83
4 - 5 %	3.13	3.51	364	9.21	3.3	1660	74.5	170	23.7	1.06	0.79
5 - 6 %	3.51	3.84	353	9.82	3.5	1580	72.5	160	22.5	1.04	0.77
6 - 7 %	3.84	4.15	343	10.2	3.7	1500	70.1	150	21.5	1.00	0.72
7 - 8 %	4.15	4.43	333	10.6	3.7	1430	68.2	140	20.4	0.975	0.69
8 - 9 %	4.43	4.71	322	10.8	3.7	1360	66.3	140	19.5	0.947	0.67
9 - 10 %	4.71	4.96	313	11.1	3.5	1300	65.3	130	18.5	0.932	0.59
10 - 15 %	4.96	6.08	285	17.2	3.7	1120	99.6	110	16.0	1.42	0.51
15 - 20 %	6.08	7.01	242	16.4	3.6	878	85.5	84	12.5	1.22	0.4
20 - 25 %	7.01	7.84	205	15.7	3.2	681	74.9	62	9.72	1.07	0.31
25 - 30 %	7.84	8.59	172	15.2	2.8	522	66.7	46	7.46	0.953	0.24
30 - 35 %	8.59	9.27	143	14.5	2.5	395	58.1	33	5.64	0.83	0.19
35 - 40 %	9.27	9.92	118	14.1	2.2	294	51.3	24	4.19	0.733	0.15
40 - 45 %	9.92	10.5	95.8	13.5	1.9	214	44.0	17	3.05	0.628	0.11
45 - 50 %	10.5	11.1	76.7	12.8	1.6	152	36.8	11	2.18	0.525	0.091
50 - 55 %	11.1	11.6	60.6	12.1	1.3	107	30.4	7.4	1.53	0.435	0.074
55 - 60 %	11.6	12.1	46.7	11.3	1.1	72.7	24.4	4.6	1.04	0.349	0.052
60 - 65 %	12.1	12.6	35.1	10.3	0.91	48.3	19.3	3.1	0.689	0.275	0.037
65 - 70 %	12.6	13.1	25.7	9.16	0.64	31.4	14.8	1.8	0.448	0.211	0.027
70 - 75 %	13.1	13.6	18.3	7.96	0.49	19.9	11.2	1.1	0.285	0.16	0.018
75 - 80 %	13.6	14.0	12.8	6.62	0.44	12.5	8.17	0.77	0.179	0.117	0.012
80 - 85 %	14.0	14.5	8.92	5.31	0.24	7.88	5.89	0.39	0.113	0.0841	0.0083
85 - 90 %	14.5	15.0	6.26	4.00	0.16	5.04	4.11	0.22	0.072	0.0588	0.006
90 - 95 %	15.0	15.7	4.42	2.89	0.13	3.25	2.80	0.14	0.0464	0.04	0.0041
95 - 100%	15.7	19.6	3.11	1.82	0.065	2.04	1.73	0.065	0.0291	0.0248	0.0027
0.0 - 2.5 %	0.00	2.47	398	8.7	1.9	1960	110	200	27.9	1.6	0.93
2.5 - 5.0 %	2.47	3.51	372	11	3.0	1720	96	1802	24.6	1.4	0.82
5.0 - 7.5 %	3.51	4.29	346	12	3.6	1520	86	150	21.7	1.2	0.74
7.5 - 10. %	4.29	4.96	320	13	3.6	1350	79	130	19.2	1.1	0.64
0.00 - 0.25 %	0.00	0.78	408	3	1.3	2070	84	210	29.6	1.2	0.98
0.25 - 0.50 %	0.78	1.10	406	3.6	1.6	2050	84	210	29.2	1.2	1.00
0.50 - 0.75 %	1.10	1.35	404	4.1	1.6	2020	84	210	28.8	1.2	0.98
0.75 - 1.00 %	1.35	1.56	402	4.6	1.6	1990	82	210	28.5	1.2	0.97

Table 1: Geometric properties (N_{part}, N_{coll}, T_{pPb}) of Pb–Pb collisions for centrality classes defined by sharp cuts in the impact parameter b (in fm). The mean values, the RMS, and the systematic uncertainties are obtained with a Glauber Monte Carlo calculation.

We use the Glauber Monte Carlo, combined with a simple model for particle production to simulate a multiplicity distribution which is then compared to the experimental one. This model is based on a number of effective number of particle-producing sources, so called ancestors, given by $N_{ancestors}$ ($N_{ancestors} = f \cdot N_{part} + (1-f) \cdot N_{coll}$). To generate the number of particles produced per interaction, we use the negative binomial distribution (NBD):

$$P_{\mu,k}(n) = \frac{\Gamma(n+k)}{\Gamma(n+1)\Gamma(k)} \cdot \frac{(\mu/k)^n}{(\mu/k+1)^{n+k}}, \tag{2}$$

which gives the probability of measuring n hits per ancestor, where μ is the mean multiplicity per ancestor and k controls the width. The simulated distribution describes the experimental one down to the most peripheral events where they start to deviate due to background contamination and limited trigger efficiency.

Figure 1 shows the distribution of V0 amplitudes for all triggered events having a vertex within 10cm, fitted by a Glauber-NBD fit.

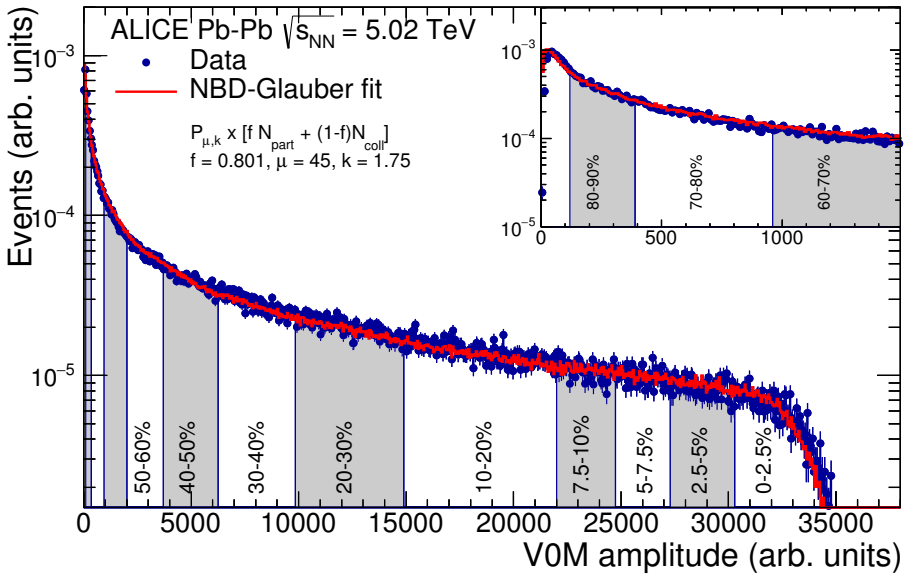

Fig. 1: (Color online) Distribution of the sum of amplitudes in the V0 scintillators. The distribution is fitted with the NBD-Glauber fit (explained in the text) shown as a line. The insert shows a zoom of the most peripheral region.

2.1 Comparison of $N_{\rm part}$ with multiplicity or impact parameter selection

We have checked the relation between geometrical parameters ($N_{\rm part}$) extracted for centrality classes selected by the impact parameter $\langle N_{\rm part}^{\rm data}\rangle$and those selected in the measured multiplicity variable $\langle N_{\rm part}^{\rm geo}\rangle$. Table 2 reports mean values and RMS for some centrality classes.

2.2 Mechanism of particle production

The number of emitting sources $N_{\rm ancestors}$ is determined by a function inspired by the two-component models, i.e. $N_{\rm ancestors} = f \cdot N_{\rm part} + (1-f) \cdot N_{\rm coll}$. However, other assumptions can be made leading to a different parametrization, which are briefly discussed in the following. The ancestor dependence on $N_{\rm part}$ and $N_{\rm coll}$ derives from a parametrization of the dependence of the charged particle multiplicity on $N_{\rm part}$ and $N_{\rm coll}$. Systematic studies of this dependence performed at the SPS [5–7], at RHIC [8], and recently at the LHC [1, 9–11], have been used in an attempt to constrain different models of particle production.

The charged particle multiplicity is expected to scale with $N_{\rm part}$ in scenarios dominated by soft processes. In this case, all the participant nucleons can be assumed to contribute with the same amount of energy to particle production, and the scaling with $N_{\rm part}$ is approximately linear. By contrast, a scaling with $N_{\rm coll}$ is expected for nuclear collisions in an energy regime where hard processes dominate over soft particle production. In this case, nuclear collisions can be considered as a superposition of binary nucleon-nucleon collisions. Two-component models are used to quantify the relative importance of soft and hard processes in the particle production mechanism at different energies.

To determine the scaling behavior of the particle production, the charged particle multiplicity $\langle {\rm d}N_{\rm ch}/{\rm d}\eta\rangle$ as a function of the number of participants $N_{\rm part}$ was fitted with a power-law function of $N_{\rm part}$ i.e.

CENT	$\langle N_{\mathrm{part}}^{\mathrm{data}} \rangle$	$\langle N_{\mathrm{part}}^{\mathrm{geo}} \rangle$	RMS data	RMS geo
0.0–0.25%	405	408	5.46	3.00
0.25–0.5%	403	406	6.66	3.60
0.5–0.75%	402	404	7.20	4.10
0.75–1%	400	402	7.99	4.60
1– 2%	395	396	9.90	6.21
2– 3%	385	386	11.6	7.49
3– 4%	374	375	12.4	8.51
4– 5%	364	364	12.8	9.21
5– 6%	353	353	12.8	9.82
6– 7%	343	343	13.0	10.2
7– 8%	333	333	12.8	10.6
8– 9%	323	322	12.8	10.8
9– 10%	313	313	12.9	11.1
10– 15%	285	285	18.2	17.2
15– 20%	242	242	16.8	16.4
20– 25%	205	205	14.9	15.7
25– 30%	173	172	13.7	15.2
30– 35%	143	143	12.1	14.5
35– 40%	118	118	10.8	14.1
40– 45%	95.9	95.8	9.69	13.5
45– 50%	76.8	76.7	8.22	12.8
50– 55%	60.8	60.6	7.23	12.1
55– 60%	46.7	46.7	6.25	11.3
60– 65%	35.1	35.1	5.21	10.3
65– 70%	25.7	25.7	4.44	9.16
70– 75%	18.2	18.3	3.65	7.96
75– 80%	12.5	12.8	2.93	6.62
80– 85%	8.29	8.92	2.28	5.31
85– 90%	5.33	6.26	1.70	4.00
90– 95%	3.26	4.42	1.17	2.89
95– 100%	2.22	3.11	0.498	1.82

Table 2: Comparison of mean and RMS for $\langle N_{\mathrm{part}}^{\mathrm{data}} \rangle$ and $\langle N_{\mathrm{part}}^{\mathrm{geo}} \rangle$. The $\langle N_{\mathrm{part}}^{\mathrm{data}} \rangle$ are calculated from the NBD-Glauber fit to the V0 amplitude, while the $\langle N_{\mathrm{part}}^{\mathrm{geo}} \rangle$ are obtained by slicing the impact parameter distribution.

Centrality	$\langle \mathrm{d}N_{\mathrm{ch}}/\mathrm{d}\eta \rangle$	$\langle N_{\mathrm{part}} \rangle$	$\frac{2}{\langle N_{\mathrm{part}} \rangle} \langle \mathrm{d}N_{\mathrm{ch}}/\mathrm{d}\eta \rangle$
0–2.5%	2035 ± 52	398 ± 2	10.2 ± 0.3
2.5–5.0%	1850 ± 55	372 ± 3	9.9 ± 0.3
5.0–7.5%	1666 ± 48	346 ± 4	9.6 ± 0.3
7.5–10%	1505 ± 44	320 ± 4	9.4 ± 0.3
0–5%	1943 ± 56	385 ± 3	10.1 ± 0.3
5–10%	1587 ± 48	333 ± 4	9.5 ± 0.3
10–20%	1180 ± 31	263 ± 4	9.0 ± 0.3
20–30%	786 ± 20	188 ± 3	8.4 ± 0.3
30–40%	512 ± 15	131 ± 2	7.8 ± 0.3
40–50%	318 ± 12	86.3 ± 1.7	7.4 ± 0.3
50–60%	183 ± 8.0	53.6 ± 1.2	6.8 ± 0.3
60–70%	96.3 ± 5.8	30.4 ± 0.8	6.3 ± 0.4
70–80%	44.9 ± 3.4	15.6 ± 0.5	5.8 ± 0.5

Table 3: The $\langle \mathrm{d}N_{\mathrm{ch}}/\mathrm{d}\eta \rangle$ and $\frac{2}{\langle N_{\mathrm{part}} \rangle} \langle \mathrm{d}N_{\mathrm{ch}}/\mathrm{d}\eta \rangle$ values measured in $|\eta| < 0.5$ for different centrality classes. We included 0–5% and 5–10%, in addition to those reported in [12]. The values of $\langle N_{\mathrm{part}} \rangle$ obtained with the Glauber model are also given. The errors are total uncertainties, the statistical contribution being negligible.

$\langle \mathrm{d}N_{\mathrm{ch}}/\mathrm{d}\eta \rangle \propto N_{\mathrm{part}}^{\alpha}$. The charged particle multiplicity per participant pair $\langle \mathrm{d}N_{\mathrm{ch}}/\mathrm{d}\eta \rangle / \left(0.5 N_{\mathrm{part}}\right)$, reported in Table 3 [12], is fitted (Fig. 2) with three different parametrizations of the ancestor dependence

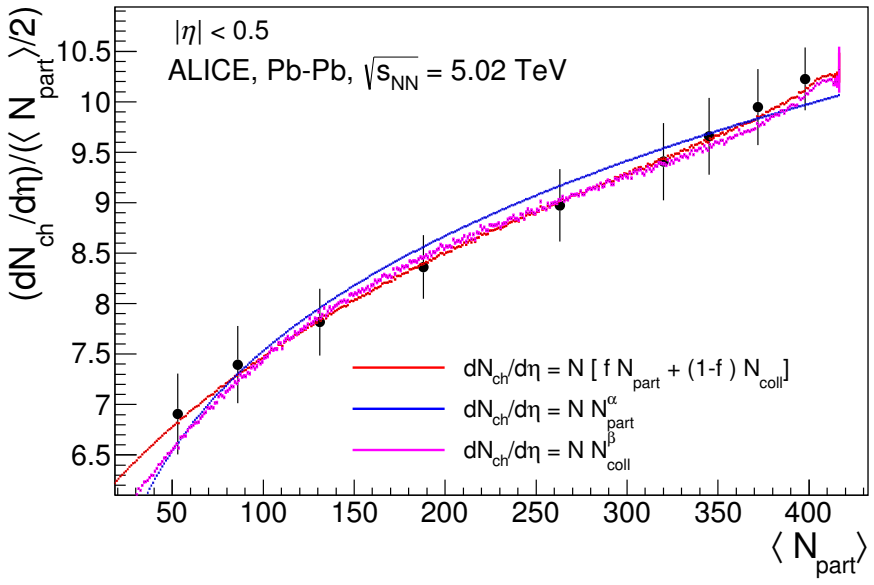

Fig. 2: (Color online) Centrality dependence of $\langle \mathrm{d}N_{\mathrm{ch}}/\mathrm{d}\eta \rangle$ per participant pair as a function of N_{part}, measured in the Pb–Pb data at $\sqrt{s_{\mathrm{NN}}} = 5.02$ TeV fitted with various parametrizations of N_{part} and N_{coll}, calculated with the Glauber model. Data are from [12].

	std Glauber	wounded quark Glauber			
	N_{part}	N_{part}		N_{cpart}/μ	
CENT	std	$N_c = 3$	$N_c = 5$	$N_c = 3$	$N_c = 5$
0 - 2.5%	398	398	398	357	433
2.5 - 5%	372	371	371	326	393
5 - 7.5%	346	344	344	298	358
7.5 - 10%	320	318	318	273	325
10 - 20%	263	260	260	218	258
20 - 30%	188	184	184	149	174
30 - 40%	131	126	126	98.6	113
40 - 50%	86.3	82.2	81.8	61.3	68.8
50 - 60%	53.6	49.9	49.5	35.4	38.6
60 - 70%	30.4	27.5	27.3	18.4	19.7
70 - 80%	15.6	13.6	13.4	8.71	8.99

Table 4: Comparison of $N_{\mathrm{part}}$from the standard Glauber in centrality classes obtained by slicing the impact parameter distribution, and from a wounded-quark Glauber MC. Two calculations of wounded-quarks have been performed, for $N_c = 3$ and $N_c = 5$ assuming a cross-section of 18 mb and 10 mb respectively.

mentioned above:

- a two-components model: $\langle \mathrm{d}N_{\mathrm{ch}}/\mathrm{d}\eta \rangle \propto f \cdot N_{\mathrm{part}} + (1-f) \cdot N_{\mathrm{coll}}$;
- a power-law function of N_{part}: $\langle \mathrm{d}N_{\mathrm{ch}}/\mathrm{d}\eta \rangle \propto N_{\mathrm{part}}^{\alpha}$;
- a power-law function of N_{coll}: $\langle \mathrm{d}N_{\mathrm{ch}}/\mathrm{d}\eta \rangle \propto N_{\mathrm{coll}}^{\beta}$.

We note that the value obtained for f is in a good agreement with the value obtained in the NBD-Glauber fit, shown in Fig. 1.

While the value obtained for α and for β with the power-law parametrization of N_{part} and N_{coll} indicate that neither of these scalings perfectly describes the data ($\alpha > 1$ and $\beta < 1$), we note that the value of α is similar to that measured at RHIC (1.16 ± 0.04 [8]) and slightly higher than that at the SPS ($\alpha \sim 1$,

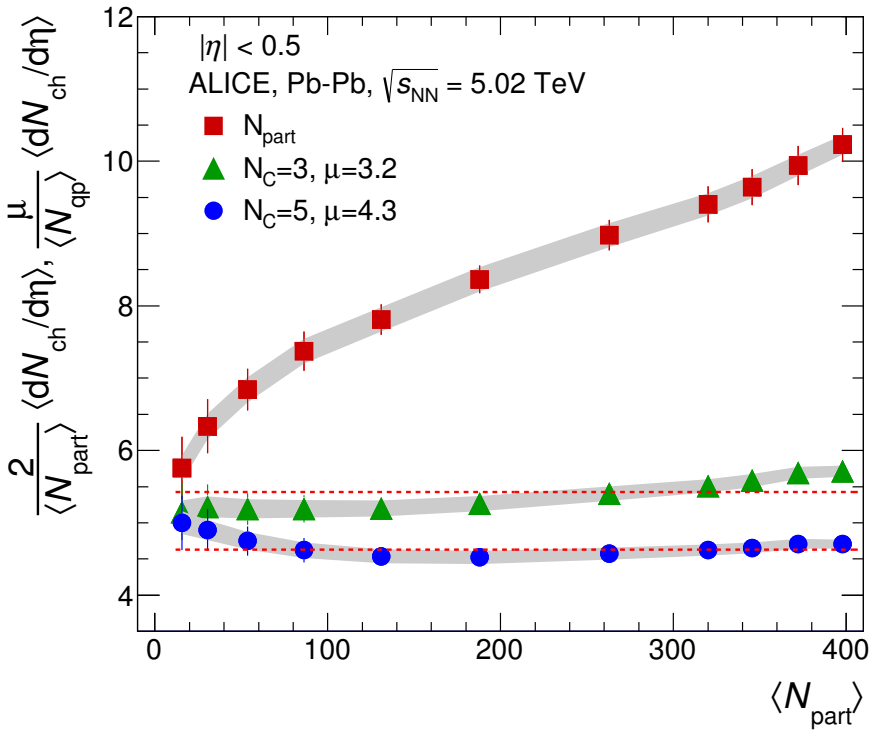

Fig. 3: (Color online) Centrality dependence of $\langle dN_{ch}/d\eta \rangle$ per participant nucleon, N_{part}, calculated with the single-quark scattering model, as a function of N_{part}, measured in the Pb–Pb data at $\sqrt{s_{NN}} = 5.02$ TeV. The $\langle dN_{ch}/d\eta \rangle$data [12] are also divided by N_{part}, calculated from the standard Glauber MC. The dashed lines indicate a fit with a constant.

see [5] for a review). The results obtained with the two-component model, where $0 < f < 1$, indicate that both the contribution of N_{part} and N_{coll} are needed to explain the particle production confirm this. However, the χ^2/NDF indicate an equally good fit for all models, thus revealing that no unique physics conclusion can be drawn from such fits and that the particular choice of parametrization has no influence on the results of the centrality determination.

2.3 Glauber Monte Carlo with quark scaling

Following [13], developed alongthe line of [14], we have also performed a Glauber calculation based on single quark scattering. Constituent quarks are located around nucleon centers with distribution

$$\rho(r) = \rho_0^{proton} \exp(-a \cdot r) \tag{3}$$

where ρ_0^{proton} is the proton radius and $a =$ is the rms charge radius of the proton. We used the often employed $N_c = 3$ for three constituent quarks as the effective number of partonic degrees of freedom, as well as $N_c = 5$. In case of $N_c = 3$ the radial distribution is modified to maintain the proton center of mass at zero and the desired radial distribution as explained in [15]. The effective q-q inelastic scattering cross section is set to 18 and 10 mb, for $N_c = 3$ and $N_c = 5$ respectively, adjusted to reproduce the 70 mb N+N inelastic cross section at 5.02 TeV. Table 4 compare the the number of participants nucleons from the standard Glauber MC with the number of participant nucleons (N_{part}) and quarks (N_{cpart}) for the extended Glauber MC. Note that N_{cpart} has been divided by $\mu = \langle N_{cpart} \rangle$ in pp collisions which is 3.4 for $N_c = 3$ and 4.3 in $N_c = 5$.

Figure 3 shows $\langle dN_{ch}/d\eta \rangle$per participant quark, calculated with the single-quark scattering model, as a function of N_{part}. The $\langle dN_{ch}/d\eta \rangle$distribution seems to scale well with the number of participating

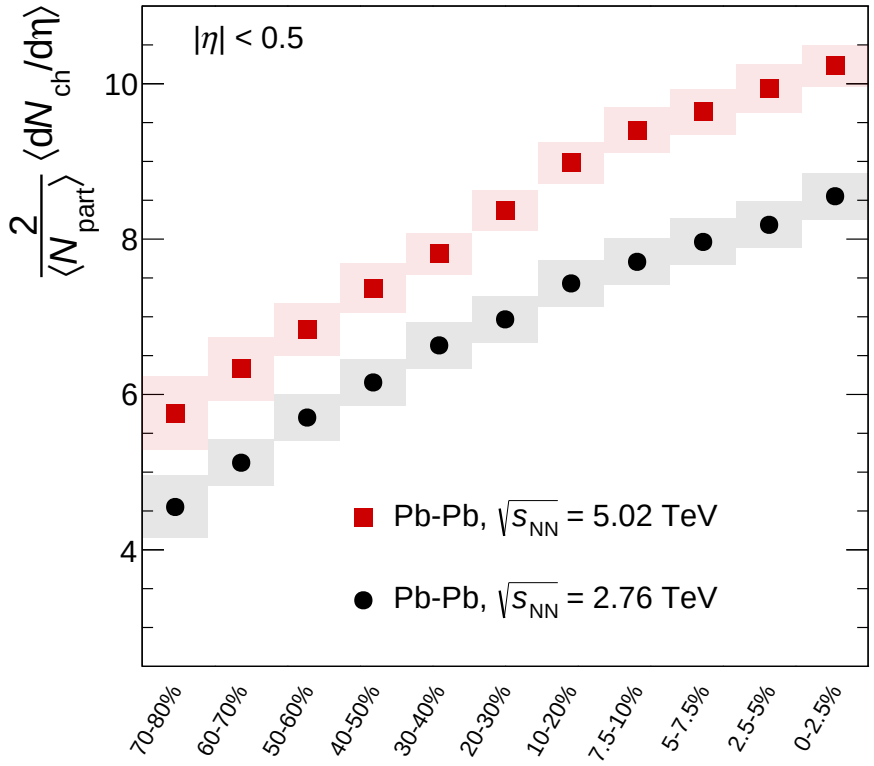

Fig. 4: (Color online) $\langle \mathrm{d}N_{\mathrm{ch}}/\mathrm{d}\eta \rangle$ as a function of the centrality classes at $\sqrt{s_{\mathrm{NN}}}$= 2.76 [9] and 5.02 TeV.

constituent quarks, as already observed in the results of PHENIX which suggested that the identical shape of the distribution indicates a nuclear-geometrical effect, well represented in terms of constituent quark participants. The results of a fit with a constant, also shown in the figure as a dashed line, indicate a better χ^2/NDF for the case of $N_c = 5$. For $N_c = 5$ the slope of a first order polinomial fit is consistent with 0.

3 Comparison of $\langle \mathrm{d}N_{\mathrm{ch}}/\mathrm{d}\eta \rangle$ at $\sqrt{s_{\mathrm{NN}}}$= 2.76 and 5.02 TeV

The centrality dependence of $\langle \mathrm{d}N_{\mathrm{ch}}/\mathrm{d}\eta \rangle$ per participant pair as a function of the number of participants N_{part} in Pb–Pb collisions measured at $\sqrt{s_{\mathrm{NN}}}$= 5.02 TeV has been compared to the same measurement performed at $\sqrt{s_{\mathrm{NN}}}$= 2.76 TeV in LHC Run 1 [9]. Figure 4 shows the results for $\langle \mathrm{d}N_{\mathrm{ch}}/\mathrm{d}\eta \rangle$ from the two analyses as a function of the centrality classes. The results at 2.76 TeV are shown with the N_{part} calculated in [1].

In order to establish an energy dependence of the centrality increase of $\langle \mathrm{d}N_{\mathrm{ch}}/\mathrm{d}\eta \rangle$ we divide the two data sets. Figure 5 shows the ratio of $\langle \mathrm{d}N_{\mathrm{ch}}/\mathrm{d}\eta \rangle$ per participant pair, $\frac{2}{\langle N_{\mathrm{part}} \rangle} \langle \mathrm{d}N_{\mathrm{ch}}/\mathrm{d}\eta \rangle$, at $\sqrt{s_{\mathrm{NN}}}$= 5.02 and 2.76 TeV. The $\langle \mathrm{d}N_{\mathrm{ch}}/\mathrm{d}\eta \rangle$ data at $\sqrt{s_{\mathrm{NN}}}$= 2.76 TeV from [9] are normalized to the N_{part} given in [1]. Because of a small change in the number of participants at the two different energies, we compare the curves as a function of centrality class. We have reanalyzed the data at $\sqrt{s_{\mathrm{NN}}}$= 2.76 TeV with the identical analysis technique used at 5.02 TeV, and the results obtained are consistent with the ones previously published in [9]. The trigger, centrality, and event-selection as well as the acceptance and efficiency for a primary particle to produce a tracklet was estimated using simulations from the same Monte Carlo generator used for the publication at $\sqrt{s_{\mathrm{NN}}}$= 2.76 TeV. In this way, some of the systematic uncertainties on $\langle \mathrm{d}N_{\mathrm{ch}}/\mathrm{d}\eta \rangle$ per participant pair cancel in the ratio. In general, the uncertainties related to the tracklet measurement are correlated in the two analyses.

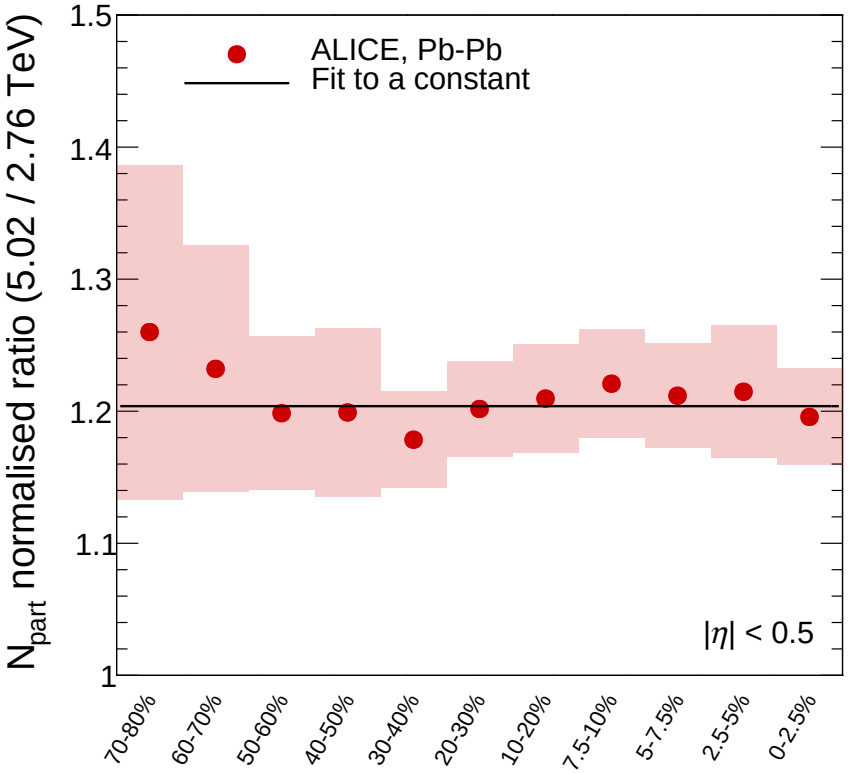

Fig. 5: (Color online) Ratio of $\langle \mathrm{d}N_{\mathrm{ch}}/\mathrm{d}\eta \rangle$ per participant pairs at $\sqrt{s_{\mathrm{NN}}}$= 2.76 [9] and 5.02 TeV, as a function of the centrality classes. The data has been normalized to N_{part} calculated from a Glauber Monte Carlo.

The subtraction of the background is performed using simulated data from the HIJING event generator [16] transported through a GEANT3 [17] simulation of ALICE and depends on the run and detector conditions. Therefore, the uncertainty attributed to the subtraction of the background, estimated injecting fake hits into real events, is, instead, uncorrelated.

Moreover, the systematic uncertainty due to the centrality class definition is not correlated. We recall that this uncertainty is estimated by using alternative centrality definitions based on SPD hit multiplicities, and by changing the fraction of the hadronic cross section used for analysis, which determines the absolute scale of the centrality (Anchor Point), within its measured uncertainty.

The determination of the Anchor Point depends mostly on the run conditions (beam-related background, EM contamination, etc [1]) and the detector conditions. Therefore it is uncorrelated in the two different energies. The correlation between the two different estimators used, namely the V0 and the SPD, is also partially related to run conditions, therefore uncorrelated. Estimators based on multiplicity at mid-rapidity are affected by a bias from multiplicity fluctuations and auto-correlations from jet-fragmentation. This was studied in details in p–Pb collisions [2]. Therefore, up to some extend, for peripheral events, the difference between estimators can be attributed to this bias. However, as the contribution of hard scattering increases with energy, this bias is energy-dependent. We therefore consider the uncertainty of the centrality estimator as largely uncorrelated at the two different energies.

The systematic uncertainties on the ratio in Figure 5 are therefore given by the quadratic sum of centrality-related uncertainties and the background subtraction uncertainties at the two energies. The statistical errors are negligible. The ratio between the data at the collisions energies shows a constant value within the uncertainties.

4 Summary

This note discusses details of the analysis of mid-rapidity pseudorapidity density of charged particles ($\langle \mathrm{d}N_{\mathrm{ch}}/\mathrm{d}\eta \rangle$) in Pb–Pb collisions at a centre-of-mass energy per nucleon pair, $\sqrt{s_{\mathrm{NN}}}$ = 5.02 TeV, which have been omitted in the publication for reasons of space.

Specifically we have provided mean numbers of the relevant geometrical quantities calculated using the Glauber Model for typical centrality classes defined by classifying the events according to their impact parameter. We have shown that they are nearly identical to those obtained with a NBD-Glauber fit to the measured multiplicity distribution. This provide a general tool to compare ALICE measurements with those of other experiments, at different energies and with different colliding systems as well as theoretical calculations.

We have also presented the comparison of $\langle \mathrm{d}N_{\mathrm{ch}}/\mathrm{d}\eta \rangle$ per participant pair as a function of the number of participants N_{part} measured at $\sqrt{s_{\mathrm{NN}}}$= 5.02 TeV to the same measurement performed at $\sqrt{s_{\mathrm{NN}}}$= 2.76 TeV. We have presented a detailed discussion of the systematic uncertainties related to the two measurements, Given that the uncertainties at the two energies are largely uncorrelated, the ratio between the data from these collision energies is consistent with being constant.

References

[1] **ALICE** Collaboration, B. Abelev *et al.*, "Centrality determination of Pb-Pb collisions at $\sqrt{s_{\mathrm{NN}}}$ = 2.76 TeV with ALICE," *Phys.Rev.* **C88** no. 4, (2013) 044909, arXiv:1301.4361 [nucl-ex].

[2] **ALICE** Collaboration, J. Adam *et al.*, "Centrality dependence of particle production in p-Pb collisions at $\sqrt{s_{\mathrm{NN}}}$= 5.02 TeV," *Phys. Rev.* **C91** no. 6, (2015) 064905, arXiv:1412.6828 [nucl-ex].

[3] **Particle Data Group** Collaboration, K. Nakamura *et al.*, "Review of particle physics," *J. Phys.* **G37** (2010) 075021.

[4] **COMPETE** Collaboration, J. C. et al., "Benchmarks for the forward observables at rhic, the tevatron-run ii, and the lhc," *Phys.Rev.Lett.* **89** no. 201801, (2002) .

[5] **NA50** Collaboration, M. C. Abreu *et al.*, "Scaling of charged particle multiplicity in Pb-Pb collisions at SPS energies," *Phys. Lett.* **B530** (2002) 43–55.

[6] **WA98** Collaboration, M. M. Aggarwal *et al.*, "Scaling of Particle and Transverse Energy Production in 208Pb+208Pb collisions at 158 A GeV," *Eur. Phys. J.* **C18** (2001) 651–663.

[7] **NA57 and WA97s** Collaboration, F. Antinori *et al.*, "Determination of the event centrality in the WA97 and NA57 experiments," *J.Phys.* **G27** (2001) 391–396.

[8] **PHENIX** Collaboration, S. S. Adler *et al.*, "Systematic studies of the centrality and s(NN)**(1/2) dependence of the d E(T) / d eta and d (N(ch) / d eta in heavy ion collisions at mid-rapidity," *Phys. Rev.* **C71** (2005) 034908, arXiv:nucl-ex/0409015 [nucl-ex]. [Erratum: Phys. Rev.C71,049901(2005)].

[9] **ALICE** Collaboration, K. Aamodt *et al.*, "Centrality dependence of the charged-particle multiplicity density at mid-rapidity in Pb-Pb collisions at $\sqrt{s_{NN}} = 2.76$ TeV," *Phys. Rev. Lett.* **106** (2011) 032301, arXiv:1012.1657 [nucl-ex].

[10] **ATLAS** Collaboration, "Measurement of the centrality dependence of charged particle spectra and RCP in lead-lead collisions at $\sqrt{s_{\mathrm{NN}}}$ = 2.76 TeV with the ATLAS detector at the LHC,".

[11] **CMS** Collaboration, S. Chatrchyan *et al.*, "Dependence on pseudorapidity and centrality of charged hadron production in PbPb collisions at a nucleon-nucleon centre-of-mass energy of 2.76 TeV," *JHEP* **08** (2011) 141, arXiv:1107.4800 [nucl-ex].

[12] **ALICE** Collaboration, J. Adam *et al.*, "Centrality dependence of the charged-particle multiplicity density at mid-rapidity in Pb-Pb collisions at $\sqrt{s_{\mathrm{NN}}}$ = 5.02 TeV," arXiv:1512.06104 [nucl-ex].

[13] C. Loizides, "Glauber modeling of high-energy nuclear collisions at sub-nucleon level," arXiv:1603.07375 [nucl-ex].

[14] S. Eremin and S. Voloshin, "Nucleon participants or quark participants?," *Phys. Rev.* **C67** (2003) 064905, arXiv:nucl-th/0302071 [nucl-th].

[15] J. T. Mitchell, D. V. Perepelitsa, M. J. Tannenbaum, and P. W. Stankus, "Tests of constituent-quark generation methods which maintain both the nucleon center of mass and the desired radial distribution in Monte Carlo Glauber models," arXiv:1603.08836 [nucl-ex].

[16] X.-N. Wang and M. Gyulassy, "Hijing: A monte carlo model for multiple jet production in pp, pa, and aa collisions," *Phys. Rev. D* **44** (1991) 3501.

[17] R. Brun *et al.*, "Geant detector description and simulation tool," *CERN Program Library Long Writeup W5013* (1994) 1–467.